

# Three-body Recombination of ${}^6\text{Li}$ Atoms with Large Negative Scattering Lengths

Eric Braaten,<sup>1</sup> H.-W. Hammer,<sup>2</sup> Daekyoung Kang,<sup>1</sup> and Lucas Platter<sup>1</sup>

<sup>1</sup>*Department of Physics, The Ohio State University, Columbus, OH 43210, USA*

<sup>2</sup>*Helmholtz-Institut für Strahlen- und Kernphysik (Theorie) and Bethe Center for Theoretical Physics, Universität Bonn, 53115 Bonn, Germany*

(Dated: December 23, 2013)

The 3-body recombination rate at threshold for distinguishable atoms with large negative pair scattering lengths is calculated in the zero-range approximation. The only parameters in this limit are the 3 scattering lengths and the Efimov parameter, which can be complex valued. We provide semi-analytic expressions for the cases of 2 or 3 equal scattering lengths and we obtain numerical results for the general case of 3 different scattering lengths. Our general result is applied to the three lowest hyperfine states of  ${}^6\text{Li}$  atoms. Comparisons with recent experiments provide indications of loss features associated with Efimov trimers near the 3-atom threshold.

PACS numbers: 31.15.-p, 34.50.-s, 67.85.Lm, 03.75.Nt, 03.75.Ss

Keywords: Degenerate Fermi gases, three-body recombination, scattering of atoms and molecules.

Atomic gases allow the experimental study of superfluidity in systems in which the fundamental interactions are simple and experimentally controllable. In the case of fermionic atoms with two spin states, there have been extensive investigations of the crossover from the *BCS mechanism* (Cooper pairing of atoms) to the *BEC mechanism* (Bose-Einstein condensation of diatomic molecules) [1]. Fermionic atoms with three spin states open up the possibility of new superfluid phases and new mechanisms for superfluidity [2, 3, 4, 5]. The first experimental studies of such a system were recently carried out using the three lowest hyperfine states of  ${}^6\text{Li}$  atoms [6, 7].

Fermionic atoms with three spin states also open up new possibilities in few-body physics. For the discussion of 3-body observables, they can simply be considered as three distinguishable atoms and their fermionic nature plays no special role. If the pair scattering lengths are large compared to the range of the interactions between the atoms, a remarkable set of 3-body phenomena are predicted. If the 3 scattering lengths are infinitely large, there is an infinite sequence of 3-atom bound states called *Efimov trimers* with a geometric spectrum and an accumulation point at the 3-atom threshold [8]. Low-energy 3-body phenomena governed by *discrete scale invariance* are generally referred to as *Efimov physics* [9, 10]. The first experimental evidence for Efimov physics were experiments with ultracold  ${}^{133}\text{Cs}$  atoms by Grimm and coworkers in which they observed dramatic dependence of the 3-body recombination rate and the atom-dimer relaxation rate on the scattering length [11, 12].

In this Letter, we present calculations of the 3-body recombination rate at threshold for distinguishable atoms with large negative pair scattering lengths in the zero-range limit. We provide semi-analytic expressions for the cases of 2 or 3 equal scattering lengths and we obtain numerical results for the general case of 3 different scattering lengths. We apply our general results to the three

lowest hyperfine states of  ${}^6\text{Li}$  atoms and compare with recent 3-body recombination rate measurements [6, 7].

We consider an atom of mass  $m$  with three distinguishable states that we label 1, 2, and 3 and refer to as spin states. We denote the scattering length of the pair  $i$  and  $j$  by either  $a_{ij} = a_{ji}$  or  $a_k$ , where  $(ijk)$  is a permutation of  $(123)$ . The rate equations for the number densities  $n_i$  of atoms in the three spin states are

$$\frac{d}{dt}n_i = -K_3 n_1 n_2 n_3. \quad (1)$$

By the optical theorem, the event rate constant  $K_3$  in the low-temperature limit can be expressed as twice the imaginary part of the forward T-matrix element for 3-atom elastic scattering in the limit where the momenta of the atoms all go to 0. Using diagrammatic methods, the T-matrix element for elastic scattering can be expressed as the sum of 9 amplitudes corresponding to the 3 possible pairs that are the first to scatter and the 3 possible pairs that are the last to scatter. For small collision energies, the leading contributions to those amplitudes come from the S-wave terms, which we denote by  $\mathcal{A}_{ij}(p, p')$ , where  $p$  ( $p'$ ) is the relative momentum between the pair that scatters first (last) and the third atom labelled  $i$  ( $j$ ). The rate constant  $K_3$  in Eq. (1) is

$$K_3 = \frac{32\pi^2}{m} \sum_{i,j} a_i a_j \text{Im} \mathcal{A}_{ij}(0, 0), \quad (2)$$

where the sums are over  $i, j = 1, 2, 3$ . The amplitudes  $\mathcal{A}_{ij}(p, p')$  can be calculated in the zero-range limit by solving 9 coupled integral equations that are generalizations of the Skorniakov–Ter-Martirosian (STM) equation [13]. To determine  $\text{Im} \mathcal{A}_{ij}(0, 0)$ , it is sufficient to solve the

9 coupled STM equations for  $\mathcal{A}_{ij}(p, 0)$ :

$$\mathcal{A}_{ij}(p, 0) = \frac{1 - \delta_{ij}}{p^2} + \frac{2}{\pi} \sum_k (1 - \delta_{kj}) \times \int_0^\Lambda dq Q(q/p) D_k(q) \mathcal{A}_{ik}(q, 0), \quad (3)$$

where

$$Q(x) = \frac{x}{2} \log \frac{1+x+x^2}{1-x+x^2}, \quad (4)$$

$$D_k(q) = (-1/a_k + \sqrt{3}q/2)^{-1}, \quad (5)$$

and  $\Lambda$  is an ultraviolet cutoff. The solutions to Eqs. (3) are singular as  $p \rightarrow 0$ . The singular terms, which are proportional to  $1/p^2$ ,  $1/p$ , and  $\ln p$ , appear only in  $\text{Re } \mathcal{A}_{ij}(p, 0)$  for real  $p$  and can be derived by iterating the integral equations [14]. Since  $\text{Im } \mathcal{A}_{ij}(p, 0)$  must be extrapolated to  $p = 0$ , it is useful to transform Eqs. (3) into coupled STM equations for amplitudes  $\bar{\mathcal{A}}_{ij}(p, 0)$  obtained by subtracting the singular terms from  $\mathcal{A}_{ij}(p, 0)$ . For  $p \ll \Lambda$ , the solutions depend log-periodically on  $\Lambda$  with a discrete scaling factor  $e^{\pi/s_0} \approx 22.7$ , where  $s_0 = 1.00624$ . The dependence on the arbitrary cutoff  $\Lambda$  can be eliminated in favor of a physical 3-body parameter, such as the Efimov parameter  $\kappa_*$  defined by the spectrum of Efimov states in the limit where all 3 scattering lengths are infinitely large [9]:

$$E_n = - \left( e^{2\pi/s_0} \right)^{-n} \frac{\hbar^2 \kappa_*^2}{m} \quad (a_{12} = a_{23} = a_{31} = \pm\infty). \quad (6)$$

If we restrict  $\Lambda$  to a range that corresponds to a multiplicative factor of 22.7, then  $\Lambda$  differs from  $\kappa_*$  only by a multiplicative numerical constant. Thus we can also simply take  $\Lambda$  as the 3-body parameter.

If  $a_{ij} > 0$ , there is a contribution to  $K_3$  from 3-body recombination into the shallow dimer whose constituents have spins  $i$  and  $j$  and whose binding energy is  $\hbar^2/(ma_{ij}^2)$ . If  $a_{12}$ ,  $a_{23}$ , and  $a_{31}$  are all negative, there are no shallow dimers. The solutions  $\mathcal{A}_{ij}(p, 0)$  to the coupled STM equations in Eq. (3) are all real-valued in this case, so the rate constant  $K_3$  in Eq. (2) is predicted to be 0.

If there are deeply-bound diatomic molecules (*deep dimers*) in any of the three 2-body channels, there are also contributions to  $K_3$  from 3-body recombination into the deep dimers. If all 3 scattering lengths are negative, these are the only contributions to  $K_3$ . The coupled STM equations in Eq. (3) do not take into account contributions from deep dimers. The inclusive effect of all the deep dimers can be taken into account by analytically continuing the Efimov parameter  $\kappa_*$  to a complex value [15]:  $\kappa_* \rightarrow \kappa_* \exp(i\eta_*/s_0)$ , where  $\eta_*$  is a positive real parameter. Making this substitution in Eq. (6), we find that the Efimov states acquire nonzero decay widths determined by  $\eta_*$ . If we use the ultraviolet cutoff  $\Lambda$  as the 3-body parameter, the inclusive effects of deep dimers

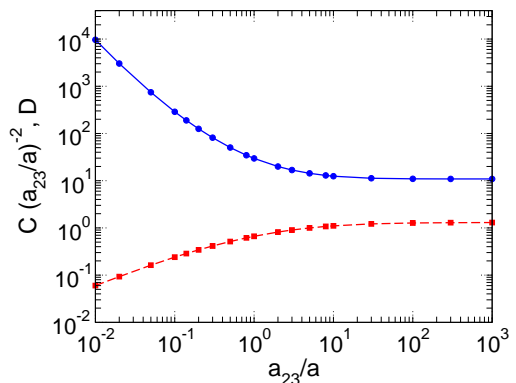


FIG. 1: (Color online) The coefficients  $C$  scaled by  $(a_{23}/a)^{-2}$  (upper curve) and  $D$  (lower curve) in Eq. (7) as functions of  $a_{23}/a$  for the case of two equal negative scattering lengths  $a$  and a third negative scattering length  $a_{23}$ .

can be taken into account by changing the upper limit of the integral in Eq. (3) to  $\Lambda \exp(i\eta_*/s_0)$ , so the path of integration extends into the complex plane. Having made this change, the solutions  $\mathcal{A}_{ij}(p, 0)$  are complex-valued even if  $a_{12}$ ,  $a_{23}$  and  $a_{31}$  are all negative. The rate constant  $K_3$  in Eq. (2) is a function of the scattering lengths  $a_{12}$ ,  $a_{23}$ , and  $a_{31}$  and the 3-body parameters  $\Lambda$  and  $\eta_*$  and it vanishes as  $\eta_* \rightarrow 0$ . It gives the inclusive rate for 3-body recombination into all deep dimers.

We focus our attention on cases in which all scattering lengths are negative, so the only recombination channels are into deep dimers. We first consider the case of 3 equal scattering lengths:  $a_{12} = a_{23} = a_{13} = a < 0$ . In this case Eq. (3) reduces – after summing over  $i$  and  $j$  – to the STM equation for identical bosons. In Ref. [15], Braaten and Hammer deduced an analytic expression for the 3-body recombination rate constant for identical bosons with a large negative scattering length  $a$ :

$$K_3 = \frac{16\pi^2 C \sinh(2\eta_*)}{\sin^2[s_0 \ln(D|a|\kappa_*)] + \sinh^2 \eta_*} \frac{\hbar a^4}{m}, \quad (7)$$

where  $s_0 = 1.00624$ ,  $C$ , and  $D$  are numerical constants. This formula exhibits resonant enhancement for  $a$  near the values  $(e^{\pi/s_0})^n (D\kappa_*)^{-1}$  for which there is an Efimov state at the 3-body threshold. Fitting our numerical results for  $K_3/a^4$  as functions of  $a\Lambda$  and  $\eta_*$ , we determine the numerical constants to be  $C = 29.62(1)$  and  $D = 0.6642(2)$ . These values are more accurate than previous results for identical bosons [9]. A separate calculation of the spectrum of Efimov states in the limit  $a \rightarrow \pm\infty$  with  $\eta_* = 0$  is necessary to determine the relation between the Efimov parameter and the ultraviolet cutoff:  $\kappa_* = 0.17609(5)\Lambda$ .

We next consider the case of 2 equal negative scattering lengths and a third that vanishes:  $a_{12} = a_{13} = a < 0$ ,  $a_{23} = 0$ . In this case with only two resonant scattering channels,  $s_0 = 0.413698$  and the discrete scaling factor

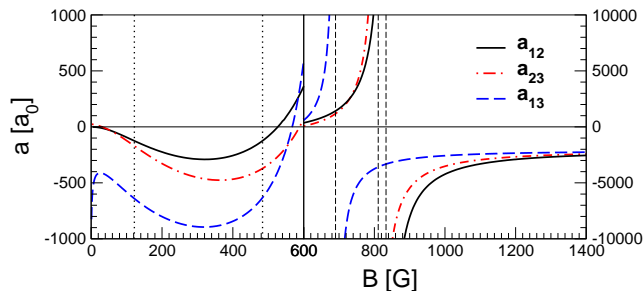


FIG. 2: (Color online) The scattering lengths for the three lowest hyperfine states of  ${}^6\text{Li}$  as functions of the magnetic field  $B$  [16]. The vertical scale changes by a factor of 10 at  $B = 600$  G. The two vertical dotted lines mark the boundaries of a region in which  $|a_{12}| > 2 \ell_{\text{vdW}}$ . The three vertical dashed lines mark the positions of the Feshbach resonances.

is  $e^{\pi/s_0} \approx 1986$ . Eq. (7) again gives an excellent fit to our numerical results and we determine the numerical constants as  $C = 0.8410(6)$  and  $D = 0.3169(1)$ .

We now consider the case of 2 equal negative scattering lengths and a third that is unequal:  $a_{12} = a_{13} = a < 0$ ,  $a_{23} < 0$ . Eq. (7) with  $s_0 = 1.00624$  continues to provide an excellent fit to our numerical results. The fitted values of  $C$  and  $D$  are shown as functions of  $a_{23}/a$  in Fig. 1. For  $|a_{23}| \gg |a|$ , the coefficients seem to have the limiting behaviors  $C \approx 10.88(2) (a_{23}/a)^2$  and  $D \approx 1.30(1)$ . Their limiting behaviors for  $|a_{23}| \ll |a|$  do not seem to be simple power laws. This is not surprising, because the discrete scaling factor 22.7 changes to 1986 when  $a_{23} = 0$ .

Finally we consider the general problem of 3 different negative scattering lengths, for which we can obtain numerical results for given values of  $a_{12}$ ,  $a_{23}$ , and  $a_{13}$ . We apply our method to  ${}^6\text{Li}$  atoms in the three lowest hyperfine states  $|f, m_f\rangle$ :  $|1\rangle = |\frac{1}{2}, +\frac{1}{2}\rangle$ ,  $|2\rangle = |\frac{1}{2}, -\frac{1}{2}\rangle$ , and  $|3\rangle = |\frac{3}{2}, -\frac{3}{2}\rangle$ . The 3 pair scattering lengths  $a_{12}$ ,  $a_{23}$ , and  $a_{13}$  are shown as functions of the magnetic field in Fig. 2 [16]. They have Feshbach resonances near 834 G, 811 G, and 690 G, respectively [17]. The zero-range approximation should be accurate if  $|a_{12}|$ ,  $|a_{23}|$ , and  $|a_{13}|$  are all much larger than the van der Waals length  $\ell_{\text{vdW}} = (mC_6/\hbar^2)^{1/4}$ , which is approximately  $62.5 a_0$  for  ${}^6\text{Li}$ . There are two regions of the magnetic field in which all 3 scattering lengths are negative and satisfy  $|a_{ij}| > 2\ell_{\text{vdW}}$ : a low-field region  $122 \text{ G} < B < 485 \text{ G}$  and a high-field region  $B > 834 \text{ G}$ . In the low-field region, the smallest scattering length is  $a_{12}$  and it achieves its largest value  $-290 a_0 = -4.6 \ell_{\text{vdW}}$  near 320 G. The zero-range approximation may be reasonable near this value of  $B$ . In the high-field region, the smallest scattering length is  $a_{13}$ . It increases from  $-3285 a_0$  at  $B = 834 \text{ G}$  to  $-2328 a_0 \approx -37 \ell_{\text{vdW}}$  at 1200 G. Thus the zero-range approximation should be very accurate in this region. We emphasize that the 3-body parameters  $\kappa_*$  and  $\eta_*$  need not be the same in the two universal regions, since there are zeroes of the scattering lengths between them.

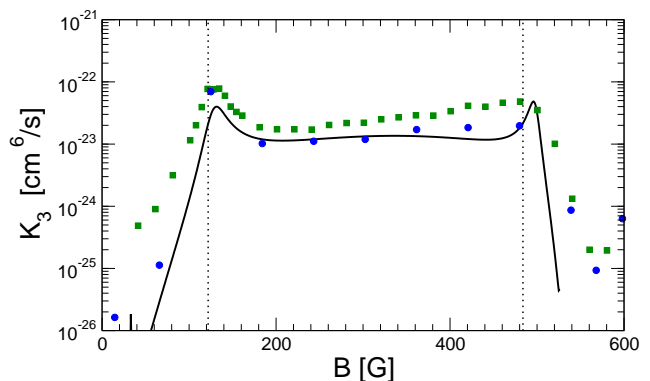


FIG. 3: (Color online) The 3-body recombination rate constant  $K_3$  as a function of the magnetic field  $B$ . The two vertical dotted lines mark the boundaries of the region in which  $|a_{12}| > 2 \ell_{\text{vdW}}$ . The solid squares and dots are data points from Refs. [6] and [7], respectively. The curve is a 2-parameter fit to the shape of the data from Ref. [6].

The 3-body recombination rate  $K_3$  for  ${}^6\text{Li}$  atoms in the three lowest hyperfine states has recently been measured by Jochim et al. [6] and by O'Hara et al. [7]. Their results are shown in Figs. 3 and 4. In Ref. [6],  $K_3$  was measured for each of the three spin states separately. Those results have been averaged to get a single value of  $K_3$  at each value of  $B$ . Both groups observed dramatic variations in  $K_3$  with  $B$ , including a narrow loss feature near 130 G and a broader loss feature near 500 G.

The narrow loss feature and the broad loss feature observed in Refs. [6, 7] appear near the boundaries of the low-field region in which all 3 scattering lengths satisfy  $|a_{ij}| > 2\ell_{\text{vdW}}$ . The zero-range approximation is questionable near the boundaries of this region. We nevertheless fit the data for  $K_3$  in this region by calculating the 3-body recombination rate using the  $B$ -dependence of  $a_{12}$ ,  $a_{23}$ , and  $a_{13}$  shown in Fig. 2, while treating  $\Lambda$  and  $\eta_*$  as fitting parameters. Since the systematic error in the normalization of  $K_3$  was estimated to be 90% in Ref. [6] and 70% in Ref. [7], we only fit the shape of the data and not its normalization. A 2-parameter fit to the data from Ref. [6] in the region  $122 \text{ G} < B < 485 \text{ G}$  gives  $\Lambda = 436 a_0^{-1}$  and  $\eta_* = 0.11$ . The fit to the shape of the narrow loss feature is excellent as shown in Fig. 3. Having fit the position and width of the loss feature feature, the normalization of  $K_3$  is determined. In the region of the narrow loss feature, the prediction for  $K_3$  lies below the data of Ref. [6] by about a factor of 2, which is well within the systematic error of 90%. The excellent fit to the shape of the narrow loss feature and the prediction of the normalization of  $K_3$  consistent with the data suggests that this loss feature may arise from an Efimov state near the threshold for atoms in spin states 1, 2, and 3. As shown in Fig. 3, our fit predicts that  $K_3$  should be almost constant in the middle of the low-field region and that there should be another narrow loss feature at

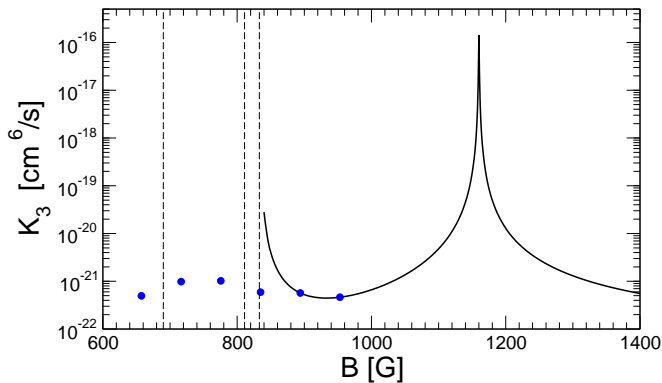


FIG. 4: (Color online) The 3-body recombination rate constant  $K_3$  as a function of the magnetic field  $B$ . The three vertical dashed lines mark the positions of the Feshbach resonances. The solid dots are data points from Ref. [7]. The curve is a 2-parameter fit to the last two data points.

its upper end near 500 G. The data from both groups in Fig. 3 increases monotonically in the middle of the low-field region and, instead of a narrow loss feature, there is a broad loss feature near the upper end of this region. We are unable to get a good fit to the slope of  $\log K_3$  in the middle of the low-field region or to the shape of the broad loss feature by adjusting  $\Lambda$  and  $\eta_*$ .

In Ref. [7], the 3-body recombination rate was also measured at higher values of the magnetic field. They include three data points in the region  $B > 834$  G, where all 3 scattering lengths are extremely large and negative. If the central values of the last two data points are used to determine the 3-body parameters, we obtain  $\Lambda = 37.0 a_0^{-1}$  and  $\eta_* = 2.9 \times 10^{-4}$ . As shown in Fig. 4, this fit predicts the resonant enhancement of the 3-body recombination rate near 1160 G. If we allow for the systematic error by increasing or decreasing both data points by 70%, the position of the resonance does not change, but  $\eta_*$  increases to  $5 \times 10^{-4}$  or decreases to  $9 \times 10^{-5}$ , respectively. If we take into account the statistical errors by increasing or decreasing the data points by one standard deviation, the position of the resonance can be shifted downward to 1109 G or upward to 1252 G. Thus it might be worthwhile to search for an Efimov resonance in this region. If such a feature were observed, measurements of its position and width would determine accurately the two 3-body parameters  $\kappa_*$  and  $\eta_*$ . Our equations could then be used to predict the total 3-body recombination rate in the entire universal region  $B > 610$  G, including the regions where 1, 2, or 3 of the scattering lengths are positive. Note that the third-to-last data point in Fig. 4 shows no sign of the large in-

crease in  $K_3$  near the Feshbach resonance at 834 G that is predicted by our fit. However the measurement of  $K_3$  involves a model for the heating of the system, and the failure of our fit at 835 G might be attributable to the breakdown of that model near the Feshbach resonance.

In summary, we have calculated the recombination rate of three distinguishable atoms with large negative pair scattering lengths in the zero-range limit. We have provided simple semi-analytical expressions for the rate if 2 or 3 scattering lengths are equal. Using our general result for 3 unequal scattering lengths, we showed that the narrow 3-body loss feature for  ${}^6\text{Li}$  atoms with three spin states [6, 7] may be attributed to an Efimov state near threshold. Our results provide a starting point for a quantitative understanding of the 3-body loss rates and the unambiguous identification of Efimov physics in these systems.

We thank S. Jochim, K.M. O'Hara, and A.N. Wenz for useful communications. This research was supported in part by the DOE under grants DE-FG02-05ER15715 and DE-FC02-07ER41457, by the NSF under grant PHY-0653312, and by the BMBF under contract 06BN411.

- 
- [1] *Ultracold Fermi Gases*, ed. M. Inguscio, W. Ketterle, and C. Salomon (IOS Press, Amsterdam, 2008).
  - [2] P.F. Bedaque and J. D'Incao, arXiv:cond-mat/0602525.
  - [3] T. Paananen, J.-P. Martikainen, and P. Törmä, *Phys. Rev. A* **73**, 053606 (2006).
  - [4] L. He, M. Jin, and P. Zhuang *Phys. Rev. A* **74**, 033604 (2006).
  - [5] H. Zhai, *Phys. Rev. A* **75**, 031603(R) (2007).
  - [6] T.B. Ottenstein, T. Lompe, M. Kohnen, A.N. Wenz, and S. Jochim, *Phys. Rev. Lett.* **101**, 203202 (2008).
  - [7] J.H. Huckans, J.R. Williams, E.L. Hazlett, R.W. Stites, and K.M. O'Hara, *Phys. Rev. Lett.* **102**, 165302 (2009).
  - [8] V. Efimov, *Phys. Lett.* **33B**, 563 (1970); *Nucl. Phys. A* **210**, 157 (1973).
  - [9] E. Braaten and H.-W. Hammer, *Phys. Rept.* **428**, 259 (2006).
  - [10] E. Braaten and H.-W. Hammer, *Annals Phys.* **322**, 120 (2007).
  - [11] T. Kraemer et al., *Nature* **440**, 315 (2006).
  - [12] S. Knoop et al., *Nature Physics* **5**, 227 (2009).
  - [13] G.V. Skorniakov and K.A. Ter-Martirosian, *Sov. Phys. JETP* **4**, 648 (1957).
  - [14] E. Braaten, H.-W. Hammer and T. Mehen, *Phys. Rev. Lett.* **88**, 040401 (2002).
  - [15] E. Braaten and H.-W. Hammer, *Phys. Rev. A* **70**, 042706 (2004).
  - [16] P.S. Julienne, private communication.
  - [17] M. Bartenstein et al., *Phys. Rev. Lett.* **94**, 103201 (2005).